Ultrasonic Determination of the Superconducting Energy Gap in Vanadium*†

JOHN L. BREWSTER,§ MOISES LEVY‡, AND ISADORE RUDNICK
Department of Physics, University of California, Los Angeles, California
(Received 20 March 1963)

Ultrasonic attenuation measurements on single-crystal cylinders axially oriented along the ⟨110⟩ crystallographic direction were used to determine the temperature-dependent superconducting energy gap $2\epsilon_0(T)$ of three samples of vanadium of different purities. An echo-pulse technique using longitudinal waves was used. The propagation direction was along the ⟨110⟩ for all the experiments. The zero-temperature energy gap for the three samples was found to be $(3.4\pm0.2)kT_c$, $(3.5\pm0.2)kT_c$, and $(3.5\pm0.1)kT_c$. These values were computed by averaging the results obtained from 200 or 300 experimental points. They are in agreement with the Bardeen, Cooper, and Schrieffer result that $2\epsilon_0(0)$ should be equal to $3.5\ kT_c$ for all superconductors. The dependence of the normalized energy gap on the reduced temperature of these samples is closely predicted by the BCS theory. These experiments were performed within the frequency range 100 to 450 Mc/sec, and in all of them the product of the ultrasonic wave vector times the electron mean free path was smaller than one. The temperature dependence of the attenuation in the superconducting state showed small oscillations. It is found that the amplitude of these is a small effect for very pure samples. Moreover, evidence has been collected to show that these oscillations are not an inherent property of the superconducting state in vanadium but are probably associated with acoustic modes of wave propagation.

INTRODUCTION

SEVERAL techniques are available for measuring the temperature-dependent energy gap of superconductors. One may determine the energy gap by means of infrared absorption,[1] by using electronic heat capacity data,[2] by thermal conductivity measurements,[3] by tunneling experiments,[4,5] and by ultrasonic attenuation measurements.[6,7] Only the latter two techniques lend themselves easily to making detailed measurements of the energy gap as a function of temperature, and the ultrasonic method has the added advantage that one can measure bulk properties of readily available sample sizes.

Bardeen, Cooper, and Schrieffer[7] (BCS) have shown that the ratio of the ultrasonic attenuation coefficient due to electron-phonon interaction in the superconducting state α_s to the coefficient in the normal state α_n is given by

$$\frac{\alpha_s}{\alpha_n}=\frac{2}{e^{\epsilon_0/kT}+1}, \tag{1}$$

where $2\epsilon_0$ is the temperature-dependent energy gap and $\epsilon_0(T)/\epsilon_0(0)$ is a universal function of the reduced temperature $T_R=T/T_c$ where T_c is the superconducting transition temperature. BCS derived Eq. (1) for longitudinal waves when the product of the ultrasonic wave number q times the electron mean free path l is much larger than 1. Tsuneto[8] and Levy[9] find that the same result holds for $ql<1$. Since

$$\epsilon_0(T)=kT\ln\left[\frac{2\alpha_n(T)}{\alpha_s(T)}-1\right], \tag{2}$$

a detailed investigation of the temperature dependence of α_s/α_n yields a detailed determination of the superconducting energy gap, $2\epsilon_0(T)$. This ratio was measured in three samples of vanadium in the frequency range 100 to 450 Mc/sec by means of a pulse-echo technique.[10]

SAMPLES

A few of the properties of the three vanadium-crystal samples are compiled in Table I. The transition temperature was determined acoustically. It was taken to be that temperature at which the ultrasonic attenuation in the sample started to decrease with decreasing temperature. The resistivity ratio—the ratio of the resistance of the sample at 300°K to the low-temperature residual resistance in the normal state—was obtained using an eddy-current technique described by Bean, DuBlois, and Nesbitt.[11] There is ample evidence, from ultrasonic measurements, that the residual resistance region extends to well above the superconducting transition temperature for all the samples and consequently the low-temperature determination was obtained just above the transition temperature. The

* Preliminary reports of this work were given at the Acoustical Society Conference, November, 1959, and the meeting of the American Physical Society, December, 1961.

† This work was supported by the Office of Naval Research.

‡ Presently a NATO Postdoctoral Fellow at the Swiss Federal Institute of Technology, Institut für kalorische Apparate und Kältetechnik, Zürich, Switzerland.

§ Present address: Field Emission Corporation, McMinnville, Oregon.

[1] P. L. Richards and M. Tinkham, Phys. Rev. **119**, 575 (1960).
[2] B. B. Goodman, paper presented at the Superconductivity Conference, Cambridge, 1959 (unpublished).
[3] A. Connolly and K. Mendelssohn, Proc. Roy. Soc. (London) **A366**, 429 (1962).
[4] I. Giaever, Phys. Rev. Letters **5**, 147, 464 (1960).
[5] J. Nicol, S. Shapiro, and P. H. Smith, Phys. Rev. Letters **5**, 461 (1960).
[6] H. E. Bommel, Phys. Rev. **96**, 220 (1954).
[7] J. Bardeen, L. N. Cooper, and J. R. Schrieffer, Phys. Rev. **108**, 1175 (1957).
[8] T. Tsuneto, Phys. Rev. **121**, 402 (1961).
[9] M. Levy, Phys. Rev. **131**, 1497 (1963).
[10] R. W. Morse, *Progress in Cryogenics* (Heywood and Company Ltd., London, 1959), Vol. I, pp. 219 ff.
[11] C. P. Bean, R. W. DuBlois, and L. B. Nesbitt, J. Appl. Phys. **30**, 1976 (1959).

TABLE I. Some properties of the three vanadium samples.

Vanadium sample	No. 1	No. 2	No. 3
Transition temperature	4.42°K	4.76°K	5.28°K
Resistance ratio	12	19	170
Diamond pyramid hardness	180	140	58
Purity	99.7	99.8	99.95
Size (diameter×length)	0.5 in.×1.00 in.	0.25 in.×1.0433 in.	0.25 in.×0.4908 in.
Axial orientation	⟨110⟩	⟨110⟩	⟨110⟩
Method of growth		Electron beam, zone refined	Electron beam, zone refined
Source	Linde Corporation	Bureau of Mines, Albany, Oregon[a]	Atomics International and Iowa State University[b]

[a] We are indebted to Lloyd Bazart, U. S. Bureau of Mines, Albany, Oregon, for supplying the vanadium No. 2 sample.
[b] The vanadium No. 3 sample was grown by H. Nadler, Atomics International, Canoga Park, California, from a polycrystalline sample obtained from Dr. F. H. Spedding, Iowa State University, Ames, Iowa.

hardness measurements were made in a Tukon Tester using a 500-g weight.

The purity of V No. 1 was assumed to be that listed by Linde Corporation. That of V No. 2 was estimated from the resistivity and hardness data.[12] The purity of V No. 3 was provided by Carlson and Owen.[13] The three crystals were grown along the ⟨110⟩ direction. This orientation was checked by x-ray diffraction and found to be accurate to within ±3°. In order to prepare the samples for measurements their ends were ground optically flat and parallel within 0.1 mil. The samples are numbered in the chronological order of their acquisition, a fact which is reflected by their successively higher purities.

GENERAL PROCEDURE

The temperature dependence of the ultrasonic attenuation coefficient of the samples is measured as follows: A 15-Mc/sec x-cut optically-polished quartz crystal is bonded[14] to one end of a properly prepared sample. The sample is then placed in a chamber which may be evacuated; see Fig. 1. The quartz crystal is excited at odd integrals of its fundamental frequency by 4–6 μsec rf pulses. The resulting ultrasonic pulses are transmitted through the sample, and after each round trip, the echo signals are received by the same quartz crystal. The resulting rf signal is detected and displayed on an oscilloscope.

Ideally one would expect the echo pulses to look as shown in Fig. 2(a). One would then measure the ultrasonic attenuation by simply fitting a logarithmic curve on top of the return pulses as shown in Fig. 2(b). Unfortunately, there usually were not enough return pulses present to permit fitting a logarithmic curve over them or the return pulse would look as shown in Fig. 2(c).

Morse[10] indicates that this nonexponential shape may be caused by insufficiently parallel faces of the sample or the quartz transducer, the probable nonuniform thickness of the ultrasonic bond, or interference between pulses traveling by different paths. On the other hand, we have found that certain characteristics of the nonexponential shape persist after regrinding the faces and rebonding the quartz, and that these characteristics differ from sample to sample. It seems likely that this can be associated with lineage, i.e., misorientation of the crystallographic axis in different portions of the sample. In these instances one cannot measure the absolute attenuation. However, since in the temperature range of these experiments the height of the received pulses is only a function of the attenuation in the sample, one may find relative changes of the absolute attenuation

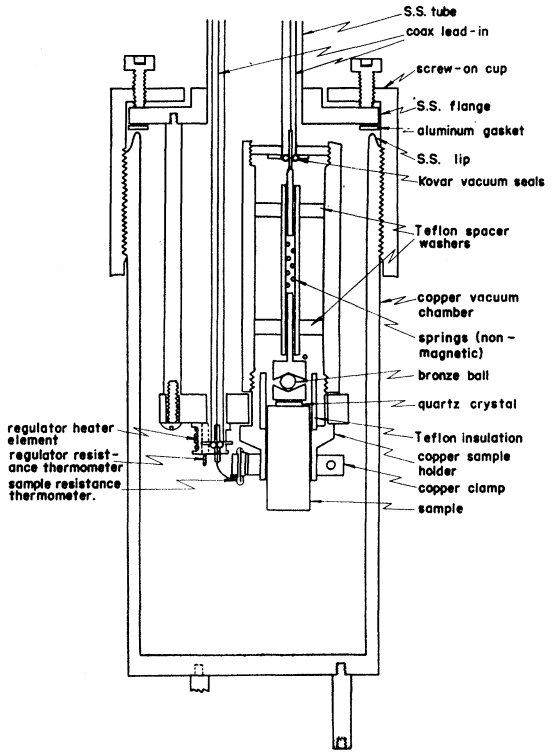

FIG. 1. Vacuum-tight sample chamber used in order to control sample temperature above the temperature of surrounding liquid helium.

[12] A. Wexler and W. S. Corak, Phys. Rev. **85**, 85 (1952).
[13] O. N. Carlson and C. V. Owen, J. Electrochem. Soc. **108**, 88 (1961).
[14] M. Levy and I. Rudnick, J. Acoust. Soc. Am. **34**, 520 (1962).

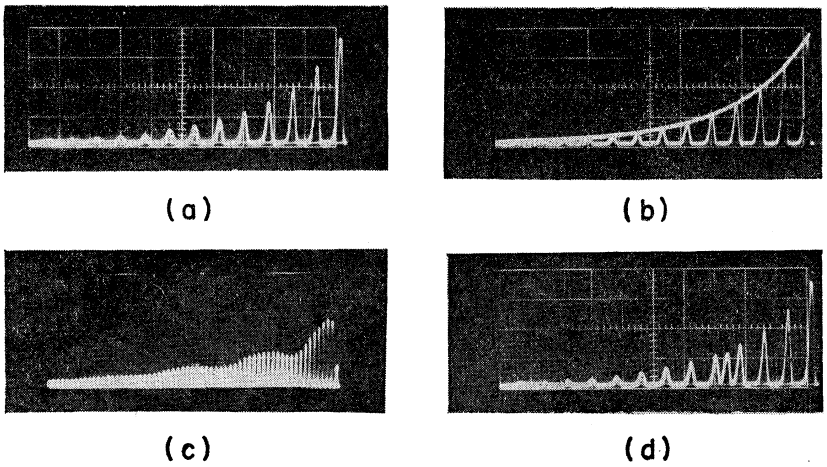

FIG. 2. Different methods of measuring changes in ultrasonic attenuation. (a) and (b) indicate the exponential-curve technique; (c) and (d), the pulse-height technique.

by measuring the change in height of one of these pulses as a function of temperature. If lineage in the sample produces refraction of the sound wave inside the sample so that its propagation direction is no longer perpendicular to the sample ends, then by elastically bending the crystal one might compensate for this refraction. Accordingly, force was applied to the middle of a sample of niobium while the ends were being supported. Figure 3 shows the height of a pulse close to a minimum in the echo pattern as a function of bending force, at 285 Mc/sec for shear pulses at room temperature. As may be seen, maximum improvement was observed for 16 lb. The shift from maximum to minimum takes about 5 lb, which is approximately the magnitude suggested by an examination of the pulse pattern of the unstressed crystal. A holder which fits in the sample chamber has been designed to apply the proper bending moment by means of springs. It is hoped that this arrangement may serve to increase the accuracy of future measurements.[15]

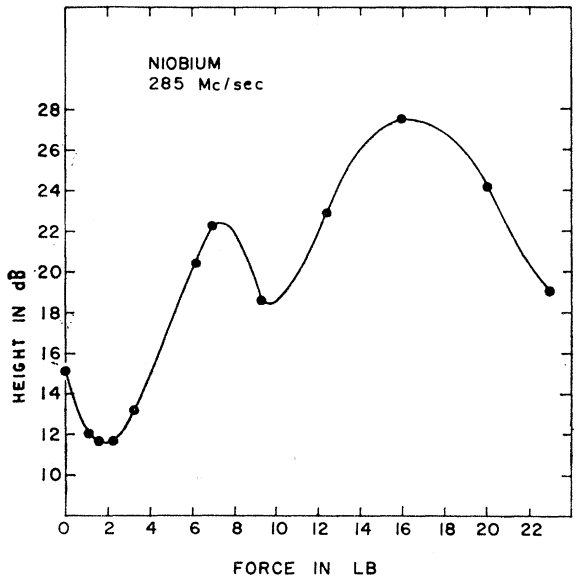

FIG. 3. Improvement of signal in Nb sample at room temperature by bending.

In order to eliminate any error due to the nonlinearity in the receiving system, a stable oscillator is used to produce a pulsed comparison signal which is transmitted through all the components of the receiving network, and with which the height of one of the return pulses is measured. An attenuator, in the comparison oscillator, enables one to visually match the height of the comparison pulse to that of the return pulse which is to be measured. Such a comparison pulse may be seen between the fourth and the fifth return pulse in Fig. 2(d). Pulse heights were read in dB.

Cryogenic temperatures are obtained by immersing the sample chamber in liquid helium at about 1.2°K. The temperature of the sample is raised above the temperature of the bath by means of an electronic temperature regulator which regulates the heat input into a block of copper surrounding the sample. The temperature is measured by means of a carbon resistor which is calibrated before each set of runs.

The ultrasonic attenuation in the normal state at temperatures below the superconducting transition temperature was obtained by quenching the superconductivity in the sample by means of a niobium superconducting magnet.[16] There was no observable change in amplitude of the pulse in the normal state; and therefore, one may conclude, as was mentioned above, that the height of the return pulses for the samples is only changed by the superconducting state of the metal, and not by any other possible sources, such as by changes of ultrasonic loss in the quartz crystal or in the bond, or by possible magnetoacoustic effects.

All the electronic equipment was regulated in order to prevent its drifting during each run—any power

[15] We are indebted to Professor R. W. Leonard for helpful discussions in connection with this effect.

[16] We are indebted to S. H. Autler, Lincoln Laboratory, MIT for providing us with the magnet.

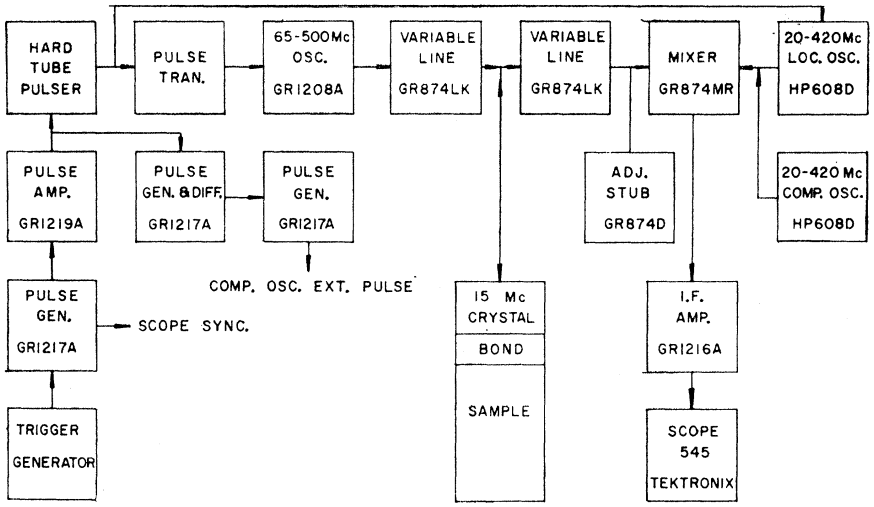

FIG. 4. Block diagram of ultrasonic equipment.

changes of the transmitter output would introduce spurious results into the height measurements of the pulses. The equipment was turned on at least 4 h before the start of the measurements. The measurements were made at successive temperatures separated by increments of about 0.02°K, while the temperature of the sample was being increased and while it was being decreased. If the upward and downward runs did not substantially agree, within either 1 or 2% of $\alpha_n L$ (L is the total length traversed by the pulse) when $\alpha_n L$ was larger than 10 dB, or within 0.1 or 0.2 dB when $\alpha_n L$ was smaller than 10 dB, then the data for that particular set of runs were discarded.

ELECTRONIC EQUIPMENT

A block diagram of the electronic equipment used for making the ultrasonic measurements is given in Fig. 4. A GR Unit pulser is triggered at 60 pulses/sec, a repetition rate that was chosen because a phase adjustment could result in minimizing 60-cps pickup problems. The 2–6 μsec pulses produced are amplified by a GR pulse amplifier to about 40 V, and then by the hard tube pulser. The resulting 2- to 4-kV pulses are inverted by a pulse transformer and then are applied to the plate of the lighthouse triode in a GR oscillator, modified to withstand the amplitude of these pulses which would otherwise cause arcing in its butterfly tuner. The GR oscillator thus produces 200 V, 4–6 μsec rf pulses, which are applied to the quartz crystal.

The same quartz crystal acts as the receiver for the reflected pulses which are then heterodyned and displayed on a scope. The local oscillator is blanked with a negative pulse from the hard tube pulser in order to avoid saturation of the 30-Mc/sec i.f. amplifier and detector by the transmitter rf pulse.

The comparison rf pulse is obtained by triggering a

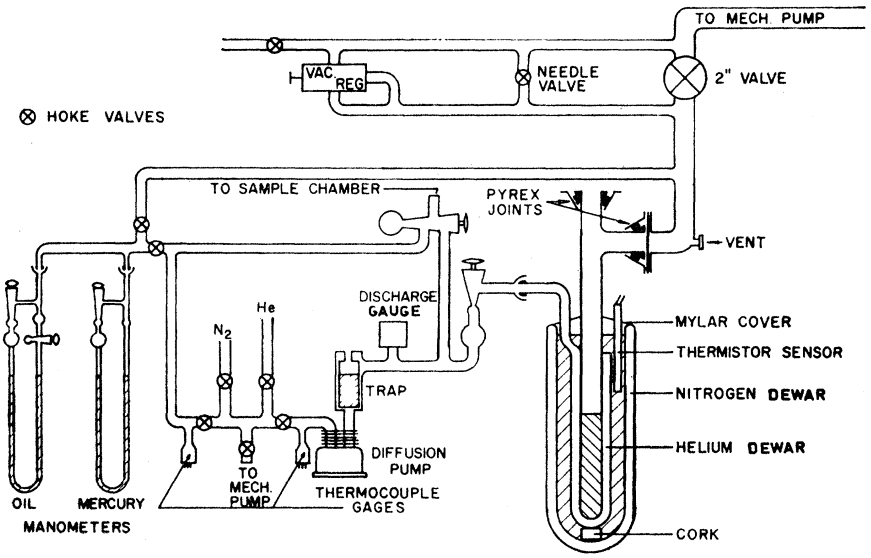

FIG. 5. Schematic of low-temperature apparatus.

Hewlett Packard 20–420-Mc/sec oscillator with a delayed positive 2-μsec pulse. For the third vanadium sample, the time between successive reflections is not long enough to permit placing a comparison pulse between them and, therefore, an interlace system was used to trigger the comparison oscillator and the transmitter on alternate sweeps of the scope.

CYROGENICS

All the ultrasonic experiments were performed in a sample chamber which was immersed in liquid helium contained in the inner Dewar of a double Dewar system. Figure 5 shows a schematic diagram of this system and the associated hardware. The jackets of the two Dewars are completely silvered except for two opposing clear vertical slits for viewing the helium level in the inner Dewar. The pressure above the liquid helium is lowered by means of a fast mechanical pump (a Beach-Russ Model 100 D; pumping rate, 100 cu ft/min) to helium pressures corresponding to about 1.2°K.

A schematic of the sample chamber is shown in Fig. 1. An aluminum flat ring lubricated with a soap-glycerine mixture is used as a gasket between the stainless steel top and the can. This arrangement is helium-II tight.

The desired temperature of the sample is obtained by achieving a balance between the cooling due to the helium bath, and the total heat input, the major portion of which is controlled by a Sommers[17] electronic thermal regulator. A power amplifier has been substituted in the last stage of this regulator. In this manner about 5 W are available for heating purposes. This maximum heat output was used for boiling off liquid nitrogen, which had been used for calibrating the carbon resistor thermometer. About 0.5 W were required to keep the sample at 10°K while the outside bath was at 1.2°K.

The regulator controls the current through a 2400-Ω wire wound resistor located about 1 in. from the axis of the sample. A $\frac{1}{2}$-W Allen-Bradley carbon resistor inside the heater is part of the bridge which is used to control the current through the heater. Thermal equilibrium of the sample to within 0.001°K is achieved in less than 15 sec.

The temperature of the sample is measured with another $\frac{1}{2}$ W 100-Ω carbon resistor located in a hole filled with vacuum grease and about $\frac{1}{2}$ in. from the axis of the sample. The thermometer resistance is measured with a GR impedance bridge, using 1 V at 500 cps as the external source. The null voltage is amplified 40 dB by a Hewlett Packard 450 AR amplifier, filtered and detected on a HP 400 C voltmeter. This method provides a temperature resolution of 5 mdeg throughout the temperature range used during these experiments.

The carbon thermometer was calibrated at the boiling point (~77°K) and the triple point (63.14°K) of nitrogen, and also at several points in liquid helium with the help of the mercury manometer. These

[17] H. S. Sommers, Jr., Rev. Sci. Instr. 25, 793 (1954).

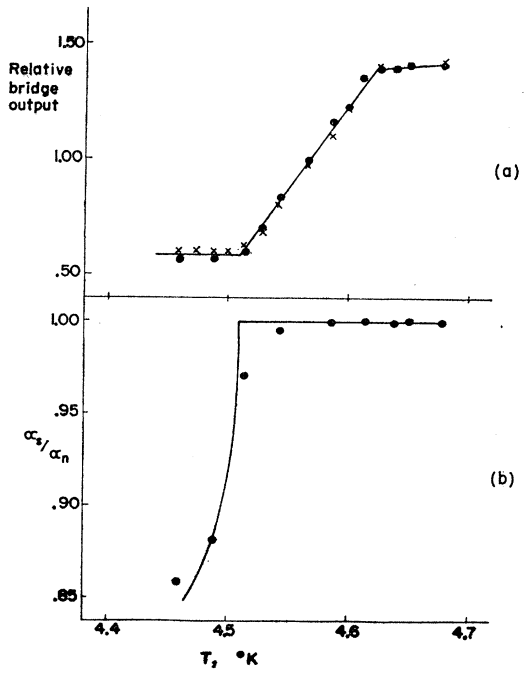

FIG. 6. Comparison of susceptibility (a) and ultrasonic (b) technique for determining superconducting transition temperature.

calibration points were used to obtain the values of the constants A, B, and K in the semiempirical equation of Clement and Quinnell,[18] relating R, the resistance of carbon resistor, to T, its absolute temperature:

$$\log_{10}R+K/\log_{10}R=A+B/T.$$

Since more than three calibration points were used, the constants were found by a least-square method. An IBM FORTRAN program[19] was used to convert the resistances to absolute temperatures.

DETERMINATION OF THE ENERGY GAP

For any particular pulse

$$\frac{\alpha_s(T)}{\alpha_n}=\frac{A(T_m)-A(T)}{A(T_m)-A(T_n)},$$

where $A(T_m)$ is the amplitude of the pulse in dB at the minimum temperature that is obtained (theoretically, this amplitude will give a value for α_s/α_n at the minimum temperature which is less than 0.005 from the value at 0°K where $\alpha_s/\alpha_n=0$); $A(T)$ = the amplitude of the pulse at the particular temperature; and $A(T_n)$ the amplitude in the normal state, a constant for each run.

As mentioned before, the transition temperature was determined by the acoustic measurements. It was taken

[18] J. R. Clement and E. H. Quinnell, Rev. Sci. Instr. 23, 213 (1952).

[19] This part of the program was obtained from G. K. Chang, IBM Research Center, Yorktown Heights, New York.

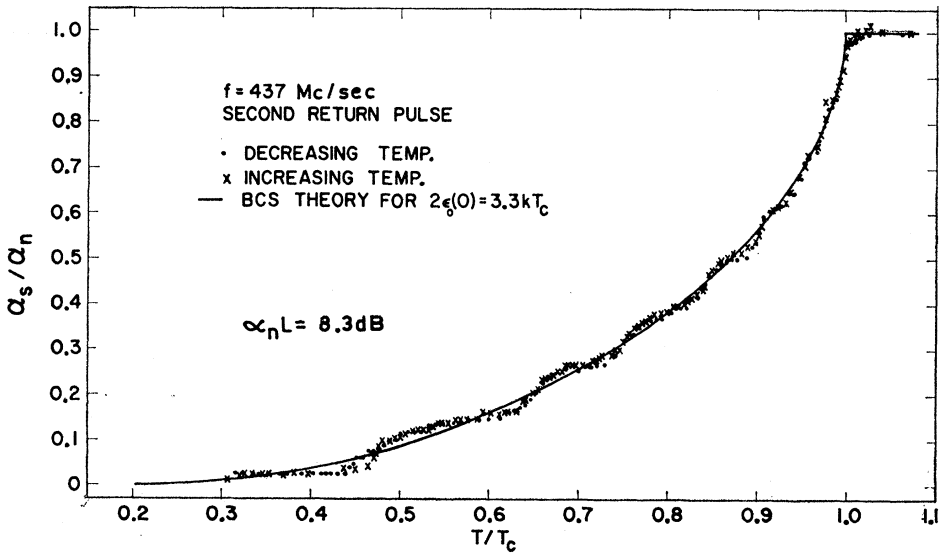

FIG. 7. Normalized attenuation as a function of reduced temperature in V No. 1 at 437 Mc/sec. This set of data clearly shows the small oscillations which have been attributed to an acoustic phenomenon.

to be equal to that temperature at which the height of the pulse started to increase sharply when the temperature was lowered slightly. An attempt was made on the first sample to correlate the ultrasonic determination of T_c with susceptibility measurements. These results are shown in Fig. 6. The discrepancy between the two measurements may be ascribed to the intermediate state. Acoustic determination of the transition temperature of V No. 3 in the absence of a magnetic field indicates that for this sample the intermediate state disappears within 0.005°K of T_c, which is within the temperature resolution of the measurements.

Once $\alpha_s(T)/\alpha_n$ is known, one may compute $[\epsilon_0(T)]_{\text{exp}}$ from Eq. (2) and find the zero-temperature energy gap $2\epsilon_0(0)$ from values of $\epsilon_0(T)/\epsilon_0(0)$ versus T_R compiled by Koppe and Miihlschlegel.[20] Since there were so many experimental points, the above computations were made by a FORTRAN program which also gave average values of $2\epsilon_0(0)$ and its mean-square deviation. This procedure was followed for evaluating the energy gap from selected runs for each sample.

The zero-temperature energy gap may also be obtained by superimposing theoretical curves[21] with different values of $2\epsilon_0(0)$ on the experimental values of $\alpha_s(T_R)/\alpha_n$ and choosing as $2\epsilon_0(0)$ that value which gives the best visual fit. This was done for all the data.

EXPERIMENTAL RESULTS

The first sample was measured at 437 Mc/sec, Fig. 7. The values of α_s/α_n are plotted against the reduced

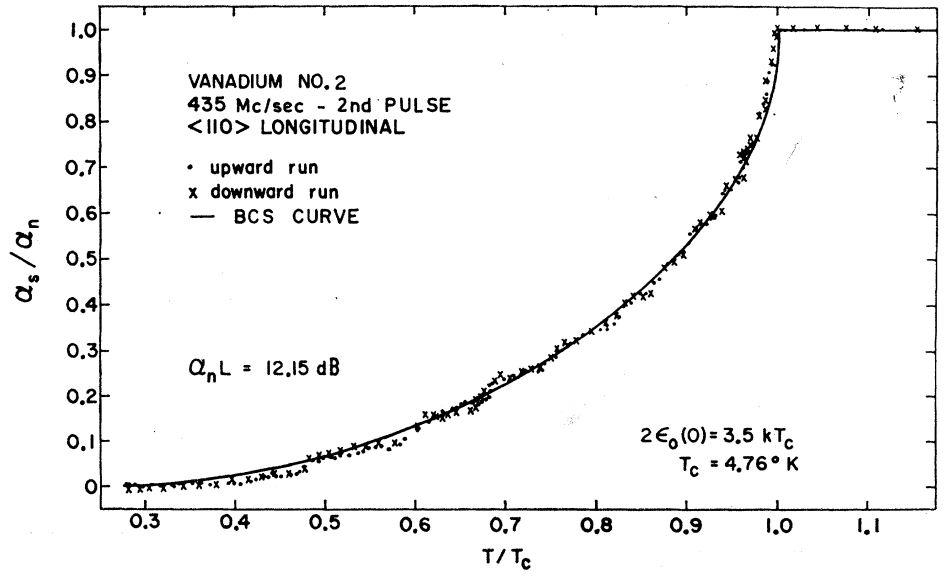

FIG. 8. Normalized attenuation as a function of reduced temperature in V No. 2 at 435 Mc/sec.

[20] Technical Report No. 13, Department of Physics, University of Illinois, Urbana, Illinois (unpublished).
[21] J. D. Gavenda (private communication).

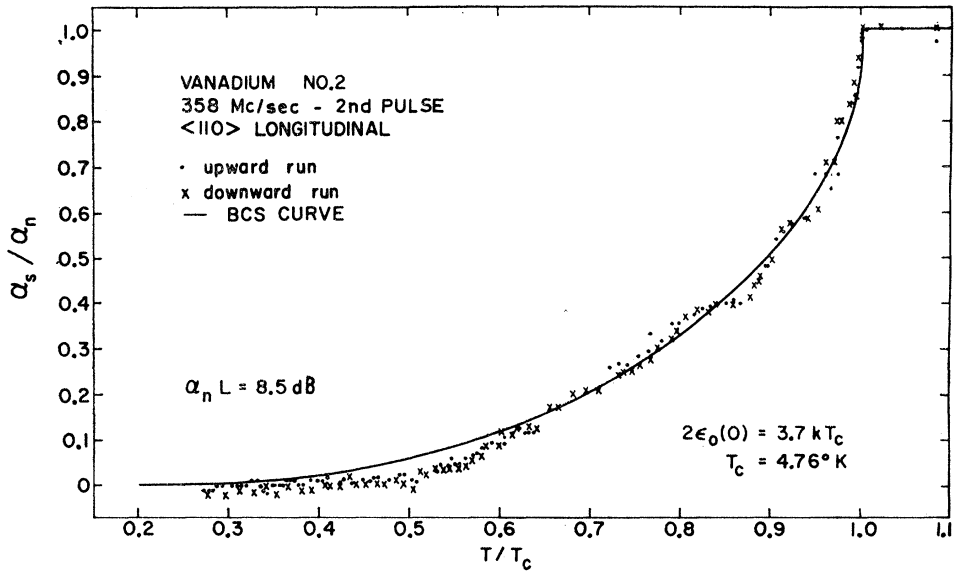

FIG. 9. Normalized attenuation as a function of reduced temperature in V No. 2 at 358 Mc/sec.

temperature, the crosses indicating points obtained while the temperature was being increased, the dots while it was being decreased. As shown in each figure, the solid line is plotted according to Eq. (1) for different zero-temperature energy gaps.

The data obtained at 437 Mc/sec were the first set that indicated the small oscillations or wiggles, about the theoretical curve. The second return pulse was measured in this case and its normal-state attenuation $\alpha_n L$ was 8.3 dB. Measurements were made on V No. 2 at three frequencies, 435 Mc/sec, Fig. 8; 358 Mc/sec, Fig. 9; 158 Mc/sec, Fig. 10. BCS curves are again superimposed on the data. The small oscillations about the mean curve are quite evident in this set of data, which spurred interest in obtaining a much purer sample of vanadium, since it was felt that perhaps the wiggles were somehow connected with the inherent properties of vanadium.

However, by the time the pure single crystal of vanadium was obtained, experiments had been performed on tantalum[22] which indicated that the wiggles were an acoustic phenomenon. A similar set of experiments was performed on the pure vanadium at 258 Mc/sec. Attenuation was measured on the third pulse, $\alpha_n L = 27.7$ dB, Fig. 11, and on the first pulse, $\alpha_n L = 9.2$ dB, Fig. 12. No evidence of wiggles is present for the third pulse; the first pulse measurements do show them. It should be pointed out, though, that if the α_s/α_n scale

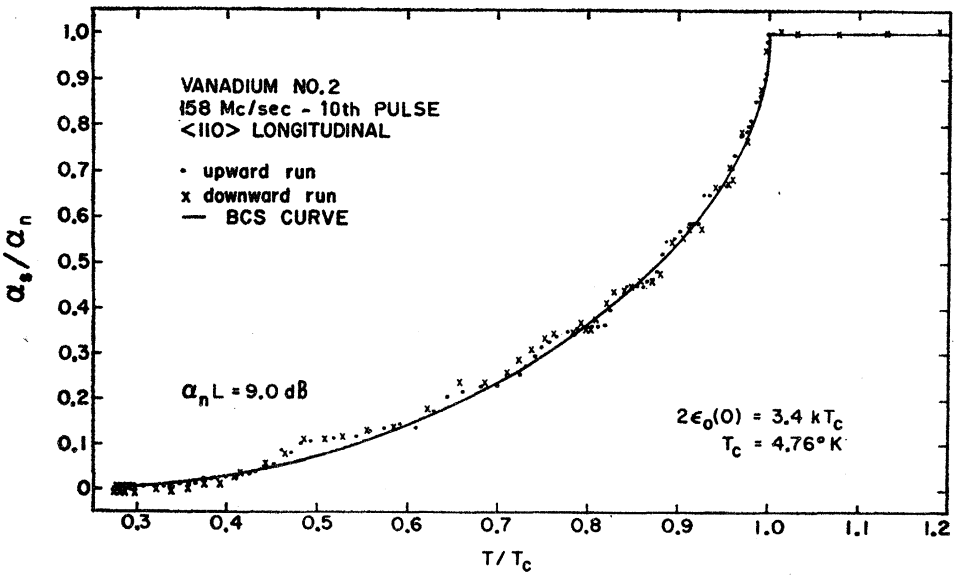

FIG. 10. Normalized attenuation versus reduced temperature for V No. 2 at 158 Mc/sec.

[22] M. Levy and I. Rudnick, following article, Phys. Rev. 132, 1073 (1963).

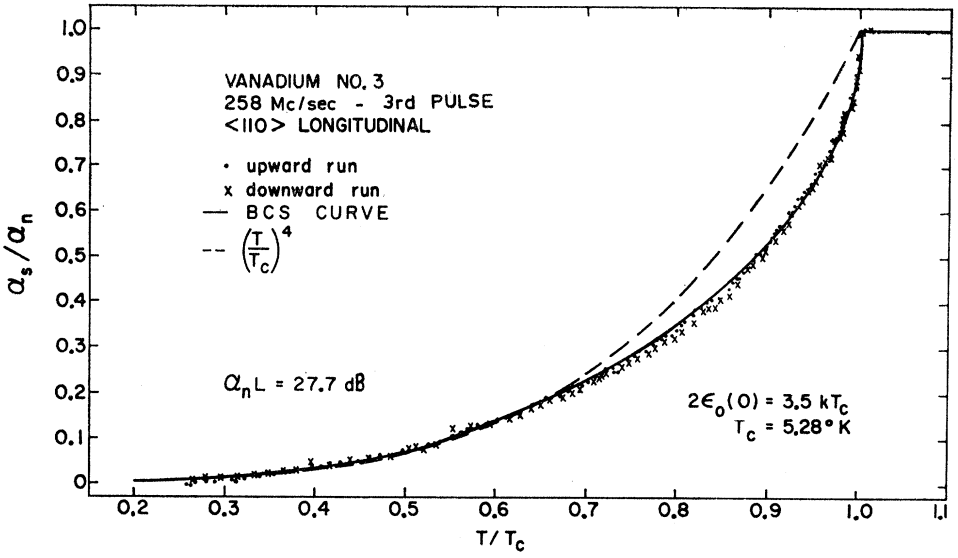

FIG. 11. Normalized attenuation versus reduced temperature for V No. 3 at 258 Mc/sec. The measurements were performed on the third pulse. These data together with those measured at the same frequency on the first return pulse, indicate that the small oscillations are an acoustic phenomenon.

for the third pulse were magnified by a factor of 3, wiggles of the same absolute size as the ones in Fig. 12 would appear. Since the curves of the normalized attenuation versus reduced temperatures for the first and third pulse did not reproduce each others shape, as regards the number and magnitude of the wiggles, it was concluded that the wiggles were neither an inherent property of vanadium nor a result of any possible intermediate state. The reproducibility of the data (during upward and downward runs) for any particular pulse eliminates the possibility that the wiggles were produced by abrupt changes in transmitter power, or by a temperature lag between the sample and the thermometer. There were no wiggles within an accuracy of 0.15 dB in the response of the comparison oscillator. Superconductivity was quenched in the second sample down to $0.65T_c$, Fig. 13. Again the ordinate is α_s/α_n, and since the pulse heights were divided by a constant α_n, it may be seen that the attenuation coefficient was also constant in this region. The same result was obtained for V No. 1 down to $0.76T_c$ and for V No. 3 down to $0.75T_c$. Therefore, the wiggles could not be ascribed to any variations in the attenuation in the normal state.

A comparison of Figs. 7, 9, and 12, wherein the total attenuation for the pulses $\alpha_n L$ is approximately the same, indicates that the absolute magnitude of the wiggles appears to depend upon the length of the samples measured. It is the same for V No. 1 and V No. 2 and only half as large for V No. 3, whose length is half of the others.

A tentative explanation for the presence of the wiggles is that since the modes comprising the longitudinal acoustic pulses have different shear compo-

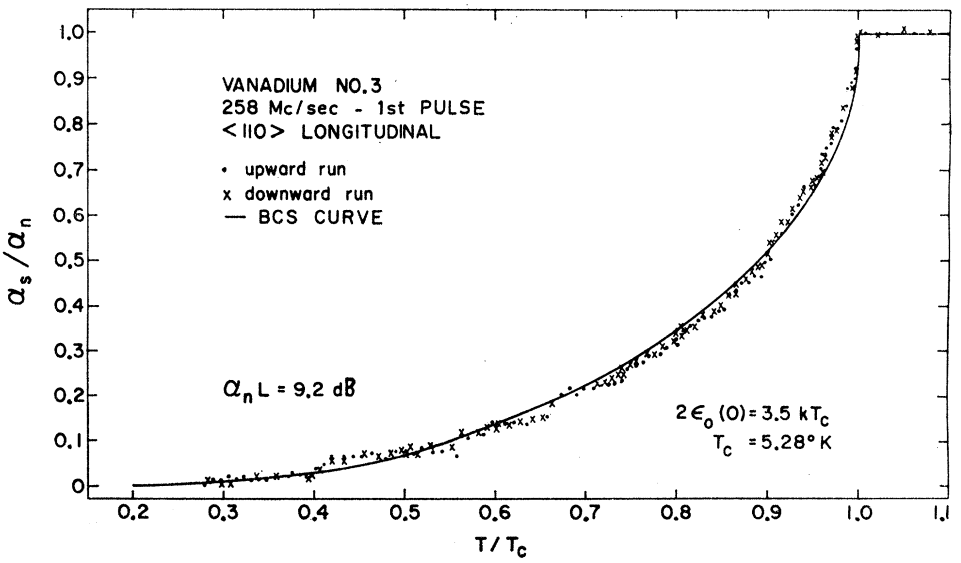

FIG. 12. Normalized attenuation versus reduced temperature for V No. 3 at 258 Mc/sec on the first return pulse. The oscillations are present here and absent in the data taken on the third pulse.

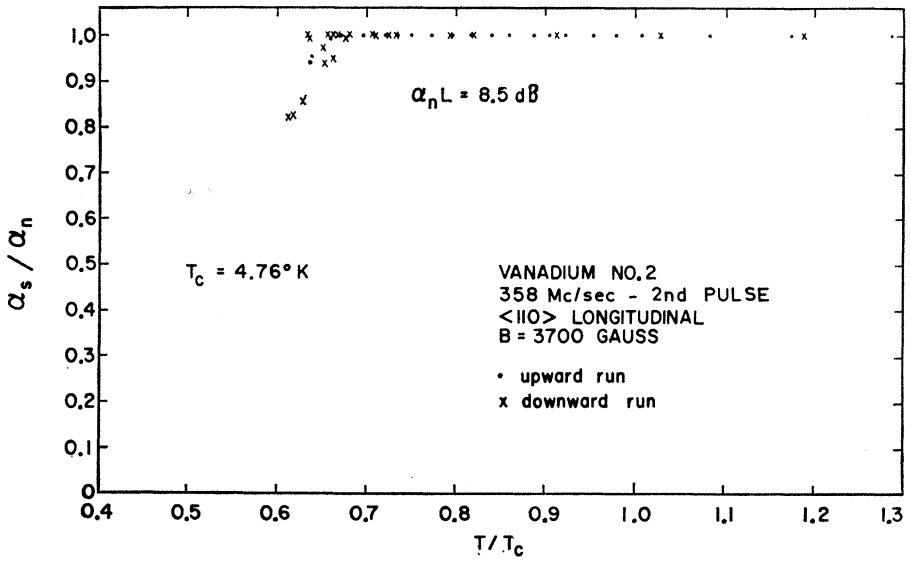

FIG. 13. Attenuation coefficient in the normal state at temperatures below T_c in V No. 2 (see text).

nents,[23] their attenuation coefficient changes at slightly different rates, and their interference could produce the wiggles, especially if one considers that the total deviation of these wiggles from the smooth theoretically predicted curve is less than 0.5 dB.

The dashed line in Fig. 11 was plotted according to the two-fluid model, which states that α_s/α_n should drop as $(T_R)^{-4}$ since the density of normal electrons is decreasing as T_R^{-4}. As may be seen, the fit is rather poor, especially near T_c.

Measurements were finally also made at 380 Mc/sec on V No. 3, Fig. 14. Points were obtained only while the temperature was being increased since the change in attenuation was large enough to make uncertainties in the pulse amplitudes unimportant especially since attention was no longer focused on the wiggles.

The magnetic field dependence of the critical temperature was measured on V No. 3. A plot of H versus $[1-T_R^2]$ is given in Fig. 15. Extrapolation of this line indicates that the critical field is 2040 G for V No. 3. This value is higher than the one reported by Corak, Goodman, Satterthwaite, and Wexler[24] for annealed high-purity vanadium, $H_c=1310$. The nature of our experimental measurement of H does not allow us to detect the deviation from the parabolic dependence predicted by BCS.

Pippard[25] has shown that in the $ql<1$ region the ultrasonic attenuation coefficient in the normal state is

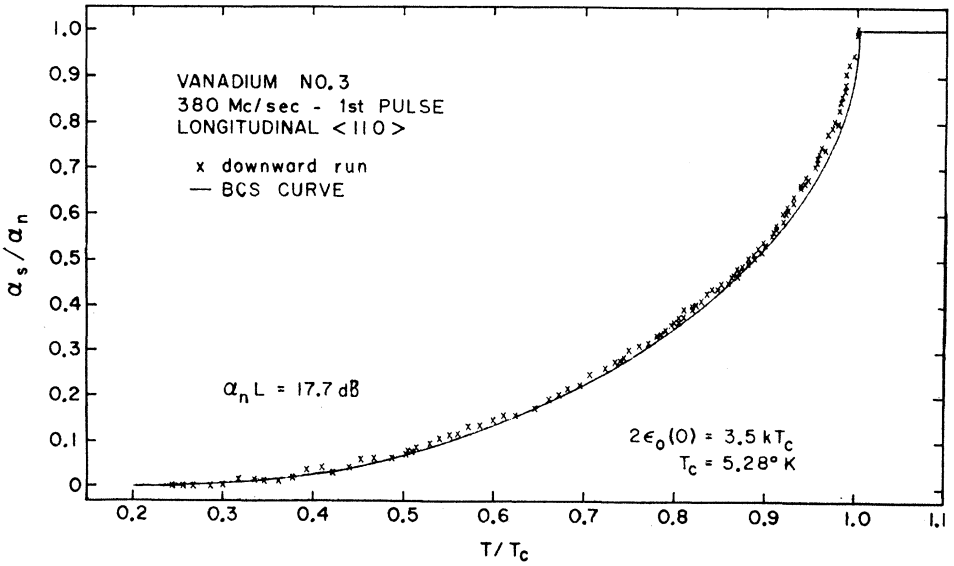

FIG. 14. Normalized attenuation versus reduced temperature for V No. 3 at 380 Mc/sec.

[23] J. Zemanek, thesis, Physics Department, University of California, Los Angeles, California (unpublished).
[24] W. S. Corak, B. B. Goodman, C. B. Satterthwaite, and A. Wexler, Phys. Rev. **102**, 656 (1956).
[25] A. B. Pippard, Phil. Mag. **46**, 1104 (1955).

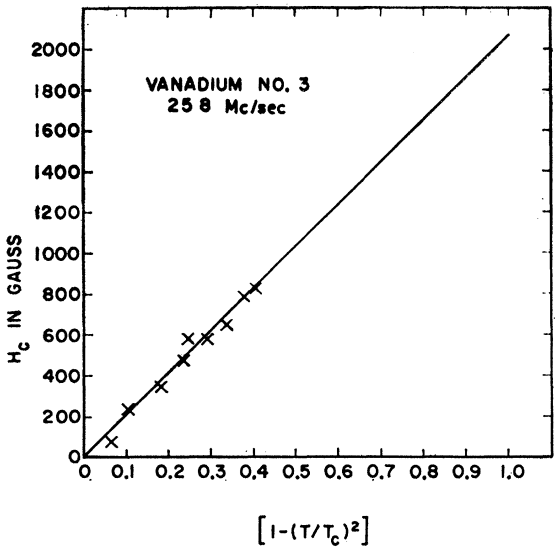

FIG. 15. Parabolic fit of critical magnetic field for V No. 3.

proportional to the square of the frequency. Figure 16 shows the frequency dependence of α_n for the three samples. Since the individual sets of points are fit by a square law, $\alpha_n \propto f^2$, one may conclude that $ql<1$.

CONCLUSIONS

Graphs of the detailed dependence of the normalized energy gap $\epsilon_0(T)/\epsilon_0(0)$ versus the reduced temperature for V No. 2 and V No. 3 are shown in Figs. 17 and 18. These figures also include the average value of the zero-temperature energy gap and its mean-square deviation as computed from all the points in each graph by the Fortran program. The solid line is the BCS result. The fit for the graphs is good above $T_R=0.5$; for values below this, the normalized attenuation has

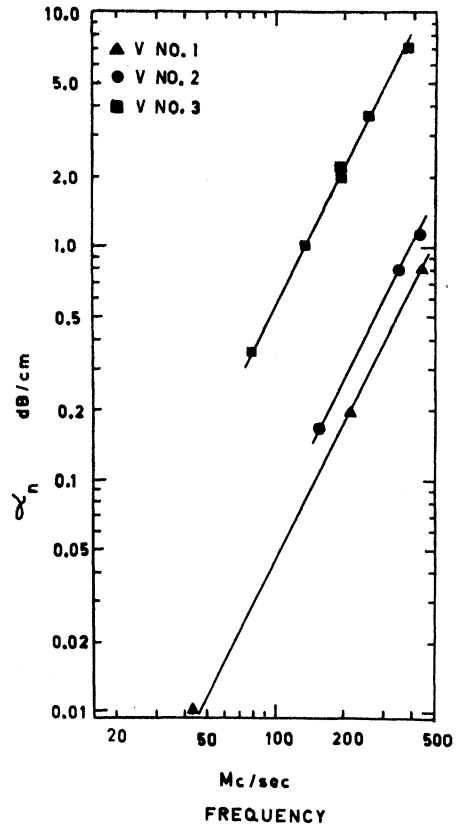

FIG. 16. Frequency dependence of the ultrasonic attenuation in the normal state for V No. 1, V No. 2, and V No. 3. The solid lines are drawn proportional to the frequency squared.

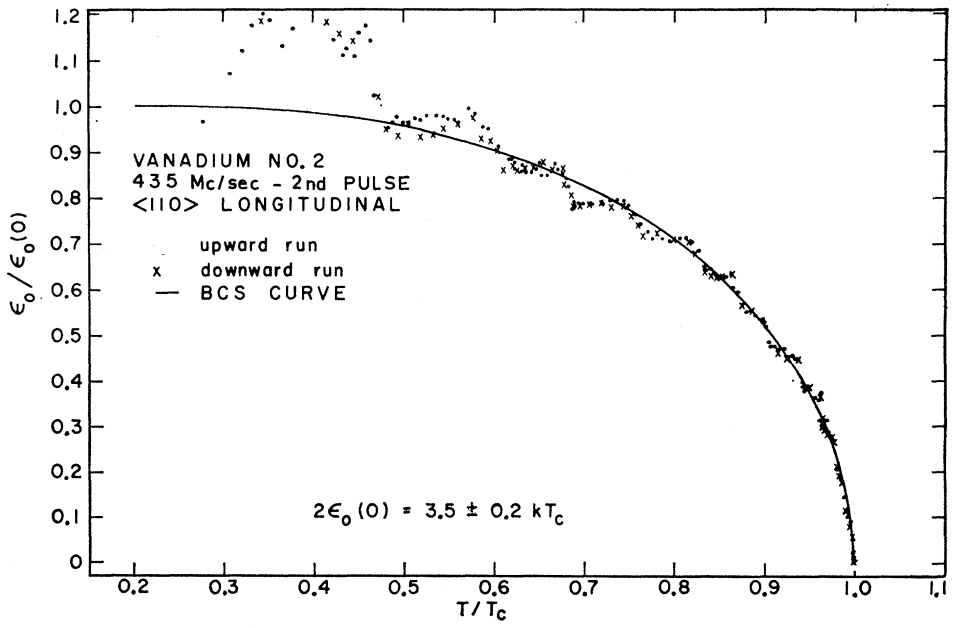

FIG. 17. Temperature dependence of the normalized superconducting energy gap in V No. 2.

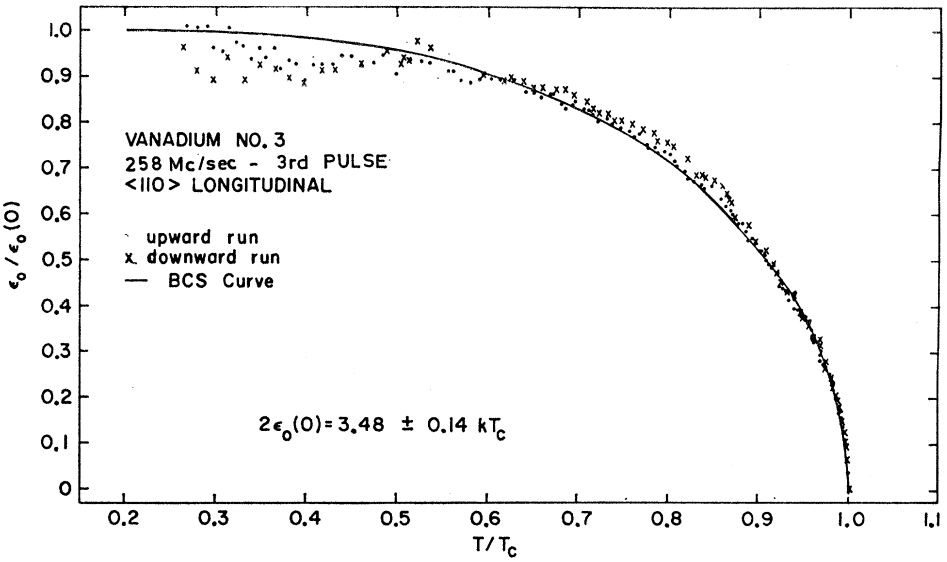

FIG. 18. Temperature dependence of the normalized superconducting energy gap in V No. 3.

dropped to a sufficiently low value, so that a small deviation from the smooth α_s/α_n versus T_R curve produces a large deviation of the energy gap, thus accounting for the relatively large scatter at the lower temperatures. A similar result is obtained for V No. 1.

Average values of $2\epsilon_0(0)/kT_c$ for the three crystals as obtained from α_s/α_n versus T_R curves together with an average deviation are shown in the first row of Table II. The second row gives the energy gap as obtained by the FORTRAN program for the best set of data in each crystal. For comparison, values of the energy gaps obtained by different techniques are also included in Table II.

The infrared absorption values were obtained by Richards and Tinkham[1] in polycrystalline vanadium.

TABLE II. Zero-temperature superconducting energy gap in vanadium in units of kT_c.

	No. 1	No. 2	No. 3
I	3.3±0.2	3.5±0.2	3.5±0.1
II	3.4±0.2	3.5±0.2	3.5±0.1
Infrared absorption		3.4±0.2	
Electron heat capacity		3.5	
Tunneling		3.4	
Ultrasonic ⟨110⟩		3.4±0.2	

Goodman's determination from electronic heat capacity was also done on polycrystalline samples.[2] Giaever[26] made the tunneling measurements in thin vanadium films. Bohm and Horwitz[27] measured the energy gap along three crystallographic orientations on a vanadium crystal with a residual resistivity ratio of 130 at 343 Mc/sec. Only the value for the ⟨110⟩ is listed.

Our measurements indicate that the superconducting zero-temperature energy gap of vanadium is $3.5kT_c \pm 0.2$, a value which is in agreement with those obtained by different techniques and with the BCS theory. The detailed temperature dependence of the energy gap of vanadium is also in agreement with the BCS theory.

ACKNOWLEDGMENTS

The authors would like to thank Reynold Kagiwada for his assistance in most of the experiments, and Professor H. E. Bommel for many helpful suggestions.

[26] I. Giaever, in *Proceedings of the Eighth International Congress on Low-Temperature Physics, London 1962* (Butterworths Scientific Publications Ltd., London, 1962).

[27] H. V. Bohm and N. H. Horwitz, in *Proceedings of the Eighth International Congress on Low-Temperature Physics, London 1962* (Butterworths Scientific Publications Ltd., London, 1962).

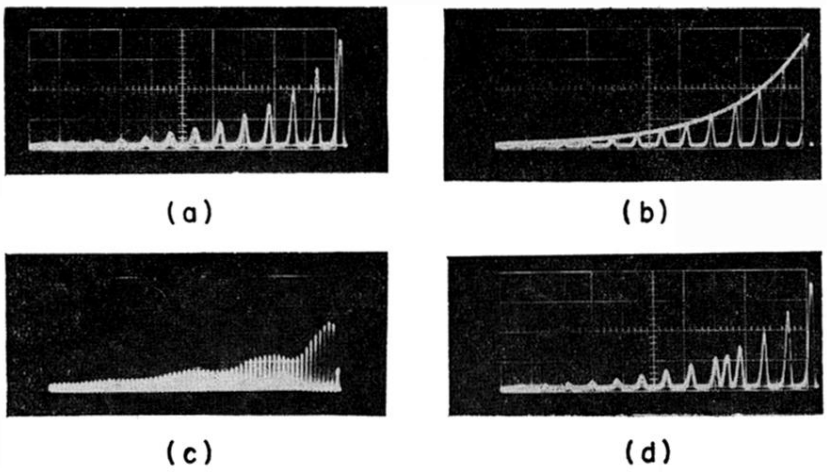

FIG. 2. Different methods of measuring changes in ultrasonic attenuation. (a) and (b) indicate the exponential-curve technique; (c) and (d), the pulse-height technique.